pH- and competitor-driven nanovalves of cucurbit[7]uril pseudorotaxanes based on mesoporous silica supports for controlled release†

Jinshui Liu and Xuezhong Du*

Received 30th July 2009, Accepted 4th January 2010
First published as an Advance Article on the web 9th March 2010
DOI: 10.1039/b915510d

The controlled release of the supramolecular nanovalves of cucurbit[7]uril (CB[7]) pseudorotaxanes based on mesoporous silica MCM-41 driven by dual stimuli were investigated in detail. The encirclement of CB[7] onto the protonated 1,4-butanediamine stalks anchored on the MCM-41 surfaces led to the tight closing of nanopores. The closed pores could be activated by the methods of deprotonation and competitive binding in aqueous media, so that the entrapped model molecules calcein were released from mesopores into bulk solutions. The nanovalve closing and opening were easily detected from the change in fluorescence intensity of calcein and even directly visualized from the change in color of dispersion solutions. The increase of pH resulted in the deprotonation of the initially protonated 1,4-butanediamine units and the dissociation of the supramolecular complexes. The amount of released calcein increased with increasing pH. The competitors cetyltrimethylammonium bromide (CTAB) and 1,6-hexanediamine could activate the nanovalves at near neutral pH through the shift of the supramolecular complex equilibrium. The increases in binding affinity and concentration of the competitors resulted in the increases of release rate and efficiency. Both of the methods could facilitate the nanovalves to realize controlled release on demand. The supramolecular nanovalves driven by a combination of deprotonation and competitive binding under various conditions will have many potential applications in different fields.

Introduction

The construction of appropriate carrier materials of active substances for controlled release is one of the major ongoing research areas in delivery systems including polymers,[1–6] dendrimeric micelles,[7] inorganic-based drug delivery systems,[8] and silica-based materials.[9–12] Among them, the mesoporous silica particles are suggested as useful carriers as a result of the excellent characteristics including good biocompatibility, high surface areas, large pore volumes, and narrow and tunable distribution of pore sizes.[13–16] These particles are amenable to surface functionalization with various organic materials, such as thiols, amines, carboxylic acids, alkoxy groups, and aromatic groups[2,17–19] by the post-synthesis grafting or co-condensation (direct synthesis) methods. The mesoporous silica-based delivery systems can be triggered by a variety of external stimuli. The controls of the access of active substances to and from mesopores have potential important applications in fluidics, sensors, and drug delivery.[12,20–22] Several research groups have reported controlled release systems based on MCM-41-type mesoporous silica with photodimerized coumarin derivatives,[23,24] photoisomerized azobenzene derivatives,[25] photochemical and chemical two-channel nanogates,[26] supramolecular hybrid gate-like ensembles,[27] and supramolecular nanovalves driven by redox,[28] pH,[29] nanoparticles,[9,30,31] and competitive binding.[32] Recently, many efforts have been devoted towards the controlled release of MCM-41-based nanovalves.[28,29,32–37] In comparison with the commonly studied controlled release without nanovalve or capping, guest molecules are released through permeability responsive to pH, ion strength, and temperature of external environments for use in sustained release.[5,6,38] However, the nanovalve-based controlled release can be applied not only for sustained release but also for rapid release in the case of emergency or targeted delivery and release. Nanovalves are machines constructed from a moving part, which consists of a macrocycle (cyclic molecule) that slides along a thread-like molecule between one or more binding stations.[28] The movable ring acts as a gate to control the access of guest molecules to and from the mesopores. When the macrocyclic molecule is positioned at the pore entrance it blocks guest molecules from entering or escaping from the interior of the pores, but when it moves off the thread or to a position far away from the pores, the guest molecules can move into or out of the pores.[28] Until now, the examples of controlled release systems that are operated by two or more stimuli in aqueous solutions are still rare[12] and remain highly desirable because most of them are operated in organic solvents.[25,28,32,33,35]

The family of cucurbit[*n*]urils (n = 5–10), abbreviated as CB[*n*]s, are very rigid cages, consisting of n glycoluril monomers joined by pairs of methylene bridges to form a rigid, annular, and hollow cavity with two highly polar carbonyl openings.[39,40] The polar carbonyl groups at the portals and the hydrophobic cavities allow CB[*n*]s to form stable host–guest complexes with small

Key Laboratory of Mesoscopic Chemistry (Ministry of Education), School of Chemistry and Chemical Engineering, Nanjing University, Nanjing, 210093, P. R. China. E-mail: xzdu@nju.edu.cn; Fax: +86-25-83317761

† Electronic supplementary information (ESI) available: Fluorescence spectra of aqueous calcein solutions at different pH and in the absence and presence of competitors at pH 6.5 and leakage of capped nanoparticles before triggered release with and without CB[7] in buffer solutions at pH 6.5. See DOI: 10.1039/b915510d

cationic molecules through the strong ion–dipole interactions. CB[*n*]s have been a target of intensive research owing to these properties.[41–43] In particular, CB[7] has attracted considerable attention because of superior solubility (20–30 mM) in aqueous solutions.[41,44,45] More recently, Stoddart and Zink *et al.* reported pH responsive supramolecular nanovalves of CB[6] pseudorotaxanes with the bisammonium stalks of 1,2,3-triazole derivatives catalyzed by the "click reaction" method and the probe molecules cationic dye rhodamine B (RhB) for monitoring nanovalve operation in aqueous solution.[36] However, it was recently reported that the fluorescence of rhodamine 6G (Rh6G), one member of the rhodamine family, was enhanced by CB[7] for use even in single-molecule detection.[45] If that is the case, cationic fluorescent dyes used would interfere with the monitoring of controlled release of the CB[*n*]-based nanovalves to some degree.

In this paper, the controlled release of CB[7] nanovalves based on MCM-41 supports with simple stalks of 1,4-butanediamine were investigated in detail. In neutral aqueous solutions, CB[7] encircled the protonated 1,4-butanediamine units tightly, thereby closing the nanopores effectively. An illustration of the functionalized MCM-41 is shown in Scheme 1. It is apparent that the CB[7]-threaded, 1,4-butanediamine stalks anchored on the surfaces of the pore interiors and around the pore entrances might act as a gate. The nanovalves could be operated by deprotonation, leading to the dissociation of the CB[7]–1,4-butanediamine supramolecular complexes and the opening of the nanovalves. Besides the routinely used method, the nanovalves could also be activated by binding of simple cationic competitors such as cetyltrimethylammonium bromide (CTAB) and 1,6-hexanediamine. Similar biologically relevant ammonium species could be produced from amino acids by decarboxylases.[46] Amino acids have low affinity to CB[7] with association constants smaller than 1×10^3 L mol^{-1}.[46] Decarboxylation produces the corresponding amines which exist in their ammonium ion forms near neutral pH[46] and thus have a very high affinity for CB[7] to facilitate a continuous dethreading of CB[7] rings from the anchored 1,4-butanediamine stalks. Herein, calcein was selected as the model molecule and could act as a fluorescence probe at the same time to monitor nanovalve operation due to its chemical and optical properties. First, calcein is an anionic fluorescent dye, and thus no interaction between calcein and CB[7] could occur, which would avoid the interference of fluorescence emission from the inclusion of cationic probe molecules inside the CB[7] cavities. Second, calcein aggregates within the mesopores only emitted weak fluorescence, but when calcein diffused into the bulk aqueous solutions it yielded strong fluorescence emission. Third, the fluorescence emission of calcein was almost insensitive to pH change and addition of competitors (CTAB and 1,6-hexanediamine). It is clear that calcein is a desirable probe molecule for the studies of controlled release in our case.

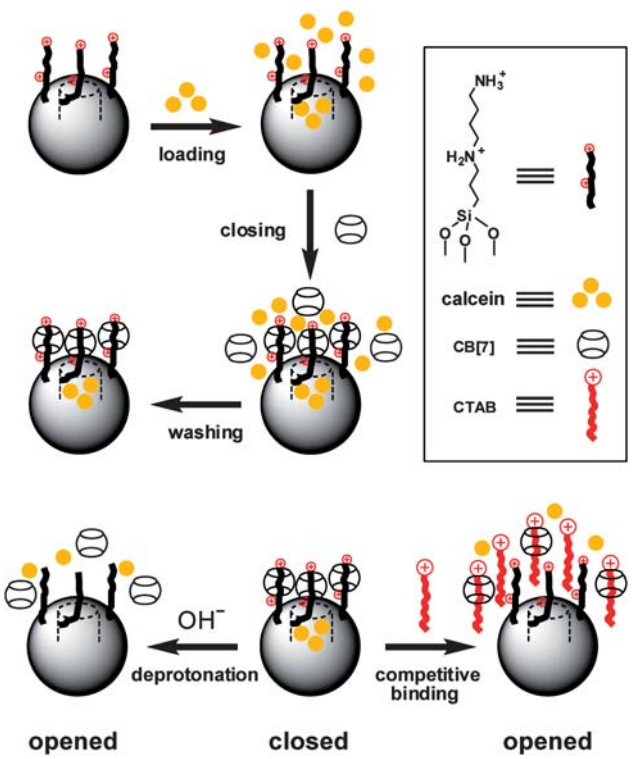

Scheme 1 Illustration of the procedures for preparation and operation of the nanovalves of CB[7] pseudorotaxanes based on mesoporous silica (not drawn to scale).

Experimental

Materials

CB[7] and CB[6] were synthesized according to the reported procedure.[47] Tetraethylorthosilicate (TEOS), 3-chloropropyltriethoxysilane (CPTES), 1,6-hexanediamine, and CTAB surfactants were purchased from Shanghai Reagent Co. (China), and 1,4-butanediamine was purchased from Alfa Aesar. Phosphate buffered saline (PBS, pH 6.5) was used in the experiments, and other basic solutions were prepared with the addition of 1.5 mol L^{-1} NaOH solution. All chemicals used were of analytical grade, and water used was double-distilled.

Preparation and modification of mesoporous silica

MCM-41-type mesoporous silica particles were prepared by the base-catalyzed sol–gel method[19,48] and used as the supports for the movable elements and the nanocontainers of the probe molecules calcein. The nanopores of MCM-41 materials were templated by CTAB, and TEOS was used as the silica precursor. Empty pores were obtained by template removal under calcination at 550 °C for 5 h. The calcined MCM-41 was dried at 150 °C over 24 h, and then chloro-functionalized MCM-41 (100 mg) was prepared by reacting with CPTES in dry toluene (15 mL) under flowing nitrogen at 95 °C for 12 h. After the reaction, the particles were filtered out and washed with methanol followed by drying under vacuum. Refluxing the CPTES-modified MCM-41 in a toluene solution of excess 1,4-butanediamine under flowing nitrogen for 12 h yielded 1,4-butanediamine-modified MCM-41. Finally, the particles were filtered out and thoroughly washed with methanol.

Calcein loading and release

The loading of calcein within the mesoporous silica particles was carried out by soaking 1,4-butanediamine-modified MCM-41 materials (20 mg) in 20 mL of PBS solution (pH 6.5) containing

calcein (2.5 mg) at room temperature for 24 h. The nanovalves were then capped upon addition of CB[7] (3.0 mg) to the system, allowing the tethered 1,4-butanediamine stalks to be encircled by CB[7] which blocked the pore entrances. The calcein-loaded, CB[7]-threaded, 1,4-butanediamine-modified MCM-41 materials were washed copiously with PBS solution (pH 6.5) to remove adsorbed calcein from the surfaces. In the course of washing and centrifugation, a slight amount of calcein could leak from the pores. The amounts of encapsulated calcein were calculated from the differences between the initial aqueous calcein solutions and the final aqueous media including the combined washing solutions after the calcein-loaded nanoparticles were removed. The loading of calcein was determined to be 4.7×10^{-6} mol g^{-1} using fluorescence spectroscopy. The resulting particles (0.05 g) after centrifugation were resuspended in 100 mL of PBS solution (pH 6.5) for the sake of steady release and monitoring. The release of calcein molecules from the nanopores was realized by adjusting the aqueous solution to the desired pH with concentrated NaOH solution or adding CTAB or 1,6-hexanediamine with different concentrations to the system.

Instruments and measurements

The specific surface area, cumulative pore volume, and pore size distribution of the MCM-41 materials were determined from nitrogen adsorption–desorption isotherms measured on an ASAP 2020 porosimeter at 77 K. The specific surface area was calculated by the Brunauer–Emmett–Teller (BET) method, and the average pore size was calculated on the adsorption branch of the isotherm using the Barrett–Joyner–Halenda (BJH) method. The ordered structure of the nanopores was confirmed by small angle powder X-ray diffraction (XRD) on a Thermo ARL SCINTAG X'TRA diffractometer using Cu-Kα radiation (λ = 0.15405 nm). The image of particle morphology was acquired using a Hitachi S-3400 scanning electron microscope (Japan). The high-resolution transmission electron microscope (HR-TEM) images were recorded on a JEM-2100 microscope. The powder samples for the HR-TEM measurements were suspended in ethanol and then dropped onto Cu grids with holey carbon films. FTIR spectra were recorded on a VECTORTM 22 FTIR spectrometer (Bruker, Germany) with KBr pellets. Steady-state fluorescence spectra were recorded on an F-4500 fluorescence spectrometer (Hitachi, Japan) with 5.0 nm bandwidth for excitation (λ_{ex} = 458 nm) and emission (λ_{em} = 520 nm).

Results and discussion

Surface functionalization of MCM-41

Nitrogen adsorption–desorption isotherms of the calcined MCM-41 materials are shown in Fig. 1a with a single and sharp adsorption step at intermediate relative pressures around 0.3. The curves can be classified as type IV isotherms according to IUPAC nomenclature associated with the nitrogen condensation inside the mesopores by capillarity. The application of the BET model resulted in a high specific surface area of 1156.1 m^2 g^{-1}. This reveals that the pores were empty after calcination so that they were accessible and suitable for use as molecular containers. The BJH method was used to obtain an average pore diameter of 2.6 nm (inset of Fig. 1a). The small angle XRD pattern of the

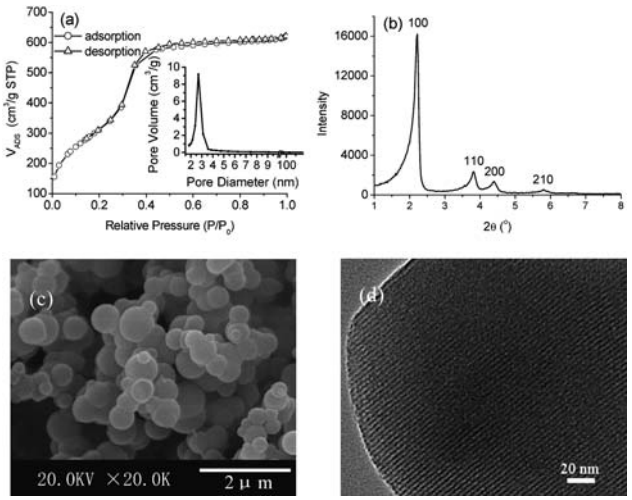

Fig. 1 (a) Nitrogen adsorption–desorption isotherms of calcined MCM-41. The inset shows pore size distribution of MCM-41; (b) small angle powder XRD pattern of calcined MCM-41; (c) SEM image of MCM-41; (d) HR-TEM image of MCM-41.

calcined MCM-41 materials in Fig. 1b shows four reflections that can be indexed as (100), (110), (200), and (210), typical of ordered two-dimensional hexagonal arrays of cylindrical pores.[48] From the XRD and porosimetry, a wall thickness of 2.0 nm could be calculated as the difference between the cell parameter $a_o = 2 \times d_{100}/\sqrt{3} = 4.6$ nm (d_{100} is the d(100) spacing) and the BJH pore diameter (2.6 nm). The scanning electron microscopy (SEM) image (Fig. 1c) shows that the silica particles were approximately spherical and had diameters ranging from 400 to 900 nm with an average of 500 nm. The HR-TEM image shows that the MCM-41 materials had typical parallel mesostructured pores (Fig. 1d). The surface functionalization of the silica particles was confirmed by FTIR spectroscopy (Fig. 2). The dominant infrared bands at 1250, 1088, and 803 cm^{-1} were due to the silica matrix of the MCM-41 materials,[27] and the bands at 3420 and 1620 cm^{-1} were related to the stretching and bending vibrations of surface hydroxyls and/or adsorbed water, respectively. The CPTES-modified MCM-41 showed a new absorption band around 2935 cm^{-1} due to the C–H stretching vibration, which indicates that CPTES molecules were tethered to the surfaces of MCM-41. For

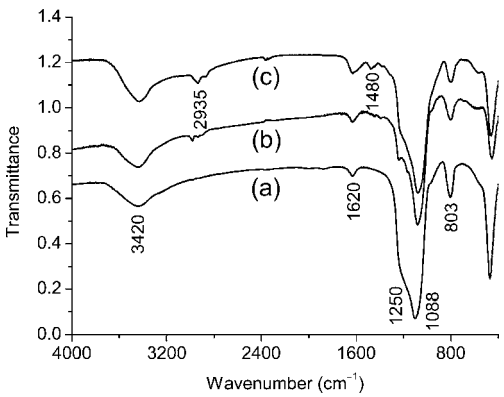

Fig. 2 FTIR spectra of (a) calcined MCM-41, (b) CPTES-modified MCM-41, and (c) 1,4-butanediamine-modified MCM-41.

the 1,4-butanediamine-modified MCM-41 the peak at 1480 cm^{-1} was indicative of the N–H bending vibration.[27]

The calcein-loaded, CB[7]-threaded, 1,4-butanediamine-modified MCM-41 materials only gave weak fluorescence owing to the self-quenching of calcein aggregates within the pores. The threading and dethreading of CB[7] onto and from the 1,4-butanediamine stalks could be controlled through pH or cationic competitors. The CB[7] rings moved away from the pore orifices and caused the opening of the nanovalves. When the nanovalves were opened, the calcein aggregates within the nanopores diffused into bulk solutions and resulted in calcein fluorescence enhancement. The controlled release of calcein was monitored by measuring luminescence intensities in response to base or competitor.

pH-driven nanovalves

The aqueous calcein solution at pH 6.5 showed a slight decrease in fluorescence intensity around 520 nm upon addition of NaOH up to pH 10.5 (Fig. S1 in ESI†). This indicates that the fluorescence emission of the aqueous calcein solution was almost insensitive to pH change from pH 6.5 to 10.5. Fig. 3 shows release profiles by plotting the fluorescence intensity at the emission maximum of calcein from the CB[7]-threaded, 1,4-butanediamine-modified MCM-41 materials in response to different pH as a function of time. Prior to base activation, the fluorescence intensities almost remained low and constant at pH 6.5, which indicates that the calcein molecules were entrapped in the nanopores of MCM-41. Near neutral pH 6.5, the 1,4-butanediamine units were in the protonated form.[46] It is well known that CB[*n*] has cation receptor properties because its carbonyl rims can stabilize positive charges through ion–dipole interactions.[39] The strong ion–dipole interaction between the CB[7] rings and protonated 1,4-butanediamine units (with an association constant of 3.7×10^5 L mol^{-1})[46] led to tight pore closing. However, the emission intensity started to increase almost immediately after increasing the pH of the aqueous system. This indicates that the calcein molecules were released from the loaded pores by means of the pH-driven dethreading of the CB[7] rings from the 1,4-butanediamine stalks. The release rate (initial curve slope) and efficiency (maximum intensity change prior to and after release) were observed to increase with increasing pH. It is shown that the association constants of the complexes of cationic guests with CB[*n*]s are much larger than those of neutral guests with CB[*n*]s.[39] It is clear that the initially protonated 1,4-butanediamine units in the near neutral aqueous solutions would be deprotonated in the basic solutions, and the supramolecular complexes of CB[7] with the 1,4-butanediamine units were accordingly dissociated. At high pH, the initially protonated 1,4-butanediamine units were totally deprotonated, resulting in the complete dissociation of the complexes of CB[7] with the 1,4-butanediamine units, the opening of the nanopore entrances, and the release of the entrapped calcein into bulk solutions. In the vicinity of the neutral conditions, the attached 1,4-butanediamine was protonated, and the modified nanoparticles were well dispersed. Upon increase of pH, originally protonated 1,4-butanediamine was gradually deprotonated, and the dispersibility of the modified nanoparticles was accordingly reduced. Precipitate might be yielded if the dispersion of nanoparticles was left for a long time at high pH, but within the timescale of controlled release here, no obvious precipitate was observed, thus there was no influence on controlled release and fluorescence monitoring upon base activation. Further increase in pH was avoided from causing probable degradation of the silica matrix. At relatively low pH, the initially protonated 1,4-butanediamine units were partially deprotonated, and the nanopores could not be completely opened or were ajar. It is clear that the release could be controlled in small portions by fine-tuning the pH of the aqueous solution. The sustained release at low pH and the rapid release at high pH could be applied to different cases, such as commonly used controlled release and emergent requirements.

Further control experiments were carried out to clarify that the calcein release were caused by the dethreading of CB[7] from the 1,4-butanediamine stalks (Fig. 4). Compared with the CB[7]-threaded, 1,4-butanediamine-modified MCM-41, the counterpart without CB[7] capping displayed no nanovalve effect. The possibility that the nanovalve effect was controlled by the anchored 1,4-butanediamine units could be eliminated. In

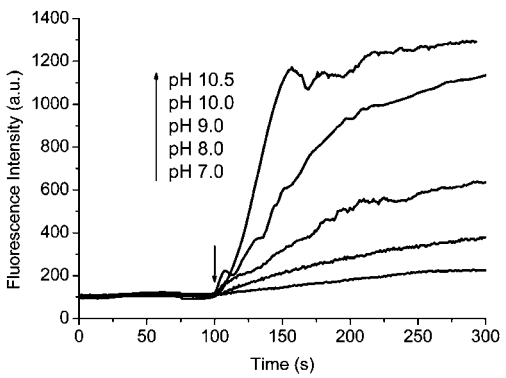

Fig. 3 Release profiles of calcein from the CB[7]-threaded, 1,4-butanediamine-modified MCM-41 systems in aqueous solutions upon base activation as a function of time at 1 s intervals. The arrow indicates that the solutions (PBS, pH 6.5) were adjusted to different pH at $t = 100$ s.

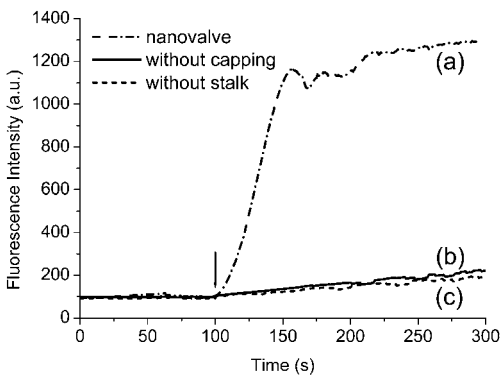

Fig. 4 Comparison of release profiles of calcein from the MCM-41 systems in aqueous solutions upon base activation as a function of time at 1 s intervals: (a) CB[7]-threaded, 1,4-butanediamine-modified MCM-41; (b) 1,4-butanediamine-modified MCM-41 without CB[7] capping; (c) MCM-41 without modification of 1,4-butanediamine in the presence of CB[7]. The arrow indicates that the solutions (PBS, pH 6.5) were adjusted to pH 10.5 at $t = 100$ s.

addition, the calcein-loaded MCM-41 materials without tethered 1,4-butanediamine stalks were investigated in the presence of CB[7]. The result showed that the nanovalve effect did not occur in this case either. The possibility that the nanovalve effect could be due to the affinity of CB[7] to the MCM-41 surfaces was ruled out. It is clear that pH-driven dethreading of CB[7] from the tethered 1,4-butanediamine units resulted in the opening of the nanovalves and the release of entrapped calcein. The initially loaded calcein in the two cases was almost leaked in the course of the washing and centrifugation at pH 6.5 because the mesopores were not capped with supramolecular nanovalves, but a small amount of calcein was still adsorbed on the surfaces or inside pores of the MCM-41 materials after copious washing because a very light colour of the dye could be observed. High pH at 10.5 could slightly promote desorption of the residual calcein from the MCM-41 materials.

At the release equilibrium, the fluorescence spectra of the aqueous systems at different pH were shown in Fig. 5a. The emission intensity of calcein was observed to increase with increasing pH. The percentage of loaded calcein released out was increased up to 92% at pH 10.5. Fig. 5b shows a plot of the amount of released calcein in fluorescence intensity as a function of pH. Interestingly, the logarithm of calcein emission intensity almost linearly increased with the increase of pH. This indicates that the release through the nanovalves could be controlled in the required portions by desired pH.

The pH-driven opening of the nanovalves could be directly visualized from color change of the suspended solutions containing the supramolecular system (Fig. 6). The calcein aggregates within the nanopores showed yellow color at pH 6.5, and

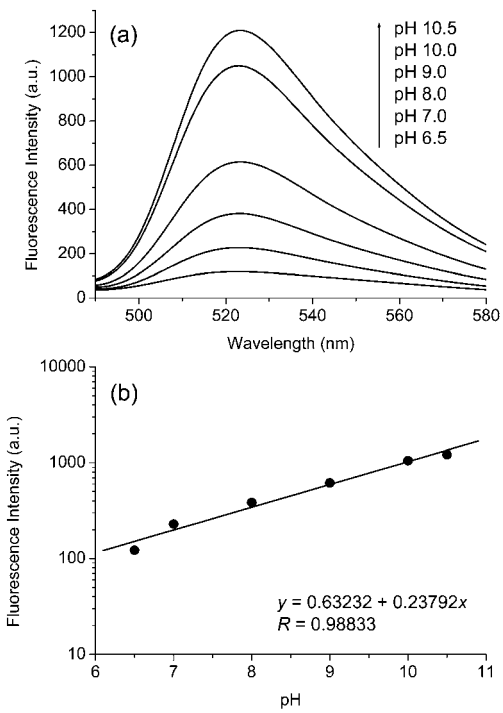

Fig. 5 (a) Fluorescence spectra of calcein released from the CB[7]-threaded, 1,4-butanediamine-modified MCM-41 systems in aqueous solutions at different pH at equilibrium and (b) emission intensity of calcein as a function of pH.

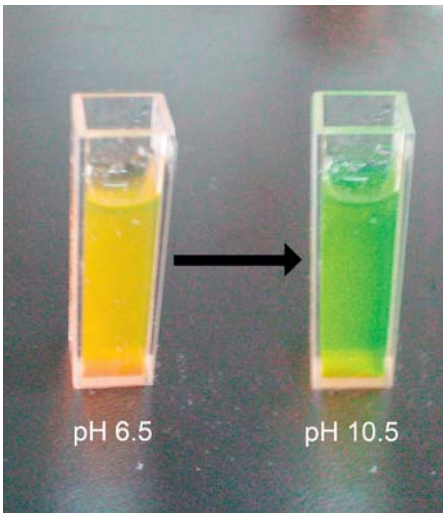

Fig. 6 Color changes of the suspended solutions containing the CB[7]-threaded, 1,4-butanediamine-modified MCM-41 system prior to and after base activation (from pH 6.5 to pH 10.5).

the suspended solution became green when the calcein molecules were released into bulk solution upon increase of pH to 10.5.

Stoddart and Zink *et al.* compared the leakage of the nanovalves of CB[6] pseudorotaxanes based on MCM-41 and indicated that short linkers between the CB[6] pseudorotaxanes and MCM-41 surfaces could tighten up the nanovalves sufficiently to prevent leakage.[36] Here, the calcein-loaded, CB[6]-threaded, 1,4-butanediamine-modified MCM-41 materials were also prepared by the same procedures for the comparison of controlled release with the CB[7]-based nanovalves (Fig. 7). Before triggered release, the emission intensity of calcein grew slowly with time in the case of CB[6]-based nanovalves rather than remaining unchanged as in the case of CB[7]-based ones. The CB[6]-based nanovalves had a relatively small amount of leakage and could not block the nanopores tightly in comparison with the CB[7]-based ones. It is known that the outer diameter of CB[7] (1.60 nm) is slightly larger than that of CB[6] (1.44 nm).[49] It is obvious that the CB[7]-based nanovalves could efficiently

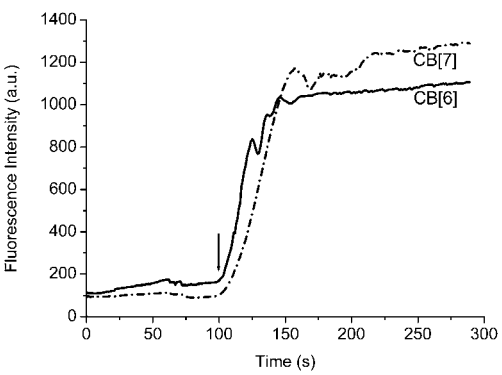

Fig. 7 Release profiles of calcein from the CB[6]- and CB[7]-threaded, 1,4-butanediamine-modified MCM-41 systems in aqueous solutions upon base activation as a function of time at 1 s intervals. The arrow indicates that the solutions (PBS, pH 6.5) were adjusted to pH 10.5 at $t = 100$ s.

block leakage to some degree taking into account the average pore diameter 2.6 nm although the BJH method usually underestimates pore sizes. On the other hand, the association constant of the complexes of CB[7] with protonated 1,4-butanediamine was reported to be approximately 3.7×10^5 L mol^{-1},[46] slightly greater than the association constant (*ca.* 1.5×10^5 L mol^{-1}) of the complexes of CB[6] with protonated 1,4-butanediamine.[50] It is clear that the relatively high binding affinities and large dimensions of the movable elements could efficiently block the pores, which resulted in no leakage before triggered release and maximum release upon activation. During the early stage of release, the rates for the CB[6]-based system was obviously faster than that for the CB[7]-based one. This was because the small dimensions of CB[6] rings and the relatively small association constant of the corresponding supramolecular complexes were favorable for nanovalve opening and calcein release. Although the absolute differences between CB[7]- and CB[6]-based nanovalves here were small, it is not difficult to understand the reason that there is no large difference in host size between CB[7] and CB[6] as a nanovalve. However, the CB[7]-based nanovalves overall exhibited superior performance of controlled release to the CB[6]-based ones in leakage resistance and release efficiency. These results indicate that the binding affinity and dimension of movable elements played important roles in controlled release of the nanovalves.

Competitive binding-driven nanovalves

The deprotonation of the protonated 1,4-butanediamine units for the disruption of the ion–dipole interactions between CB[*n*] and 1,4-butanediamine stalks was the common method for the dethreading of the macrocycles and opening of the nanovalves. In addition, the nanovalves could be activated by competitive binding for the macrocycles at constant pH through the shift of the supramolecular complex equilibrium. The operation of the nanovalves by competitive binding would broaden their potential applications.

CTAB and 1,6-hexanediamine were selected to investigate the competitive binding mechanism due to their different binding affinities to CB[7] (Fig. 8). CTAB is a cationic surfactant and can form a stable complex with CB[7]. The association constant of the CB[7] complexes with alkyltrimethylammoniums was approximately 5.8×10^5 L mol^{-1}.[51] The protonated 1,6-hexanediamine has two cations and an alkyl chain of suitable length with a high binding affinity to CB[7], thus its association constant was as large as $(8.97 \pm 1.43) \times 10^7$ L mol^{-1}.[52] When CTAB was added to the calcein-loaded, CB[7]-threaded, 1,4-butanediamine-modified MCM-41 system at pH 6.5, the fluorescence intensity of calcein increased obviously, which indicates that the calcein molecules were released from the nanopores into bulk solutions. This reflects that CTAB facilitated the dissociation of the CB[7]–1,4-butanediamine complexes and then was included into the CB[7] cavities. The newly formed inclusion complexes of CTAB with CB[7] were far away from the MCM-41 surfaces and were dispersed in aqueous solution, thus the nanovalves were simultaneously opened. An increase in CTAB concentration resulted in the increase of release rate and efficiency of calcein. The increase of CTAB concentration could give rise to the shift of the supramolecular complex equilibrium because the association constant of the CB[7] complex with alkyltrimethylammoniums (5.8×10^5 L mol^{-1})[51] was very comparable to that of the CB[7] complex with protonated 1,4-butanediamine (3.7×10^5 L mol^{-1}).[46] Furthermore, the release rate and efficiency in the presence of protonated 1,6-hexanediamine were much larger than those in the case of CTAB when the two competitors were present at the same concentrations. The release efficiencies at the given competitor concentration of 1.0×10^{-4} mol L^{-1} were determined to be 66% for CTAB and 73% for 1,6-hexanediamine. It could be concluded that release rate and efficiency were dependent not only on concentration of the competitors but also on binding affinity of the competitors for the movable elements. These results indicate that strong binding affinity between the competitors and movable elements was even more significant than the increase of competitor concentrations for nanovalve activation.

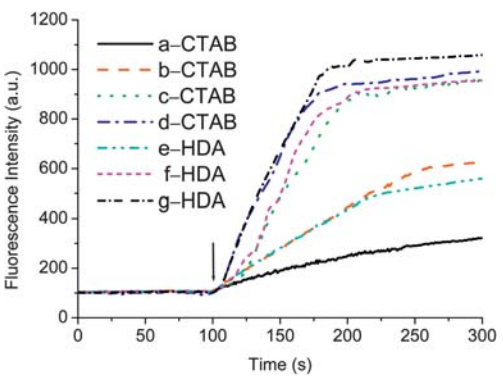

Fig. 8 Release profiles of calcein from the CB[7]-threaded, 1,4-butanediamine-modified MCM-41 systems in aqueous solutions (PBS) at pH 6.5 driven by competitive binding as a function of time at 1 s intervals; CTAB/10^{-4} mol L^{-1}: a) 0.2; b) 0.6; c) 1.0; d) 5.0; 1,6-hexanediamine (HDA)/10^{-4} mol L^{-1}: e) 0.2; f) 0.6; g) 1.0. The arrow indicates the addition of competitors to the solutions at $t = 100$ s.

Although calcein is an anionic dye, both CTAB and 1,6-hexanediamine displayed a slight influence on fluorescence emission of aqueous calcein solutions (Fig. S2†). However, the fluorescence of the calcein-loaded, CB[7]-threaded, 1,4-butanediamine-modified MCM-41 system was considerably enhanced upon introduction of CTAB or 1,6-hexanediamine (Fig. 9a and b) because the calcein molecules were released into bulk solution. CTAB and protonated 1,6-hexanediamine competed with the protonated 1,4-butanediamine units for CB[7], leading to the dethreading of CB[7] from the 1,4-butanediamine stalks and the opening of the nanovalves. The amount of released calcein (the emission intensity at equilibrium) as a function of concentration of the competitors added is shown in Fig. 9c. The plots showed Langmuir-like type curves, and their linear relationship was existent for competitor concentrations at least up to 6×10^{-5} mol L^{-1}. These indicate that in the concentration range the release could be precisely controlled by varying concentrations of different competitors.

The CB[7] pseudorotaxanes used here were stable, but not kinetically stable because of host dissociation. In this regard, considering that the association constant of the complexes of CB[7] and protonated 1,4-diaminobutane was 3.7×10^5 L mol^{-1},[46] when the capped nanoparticles were exposed to PBS

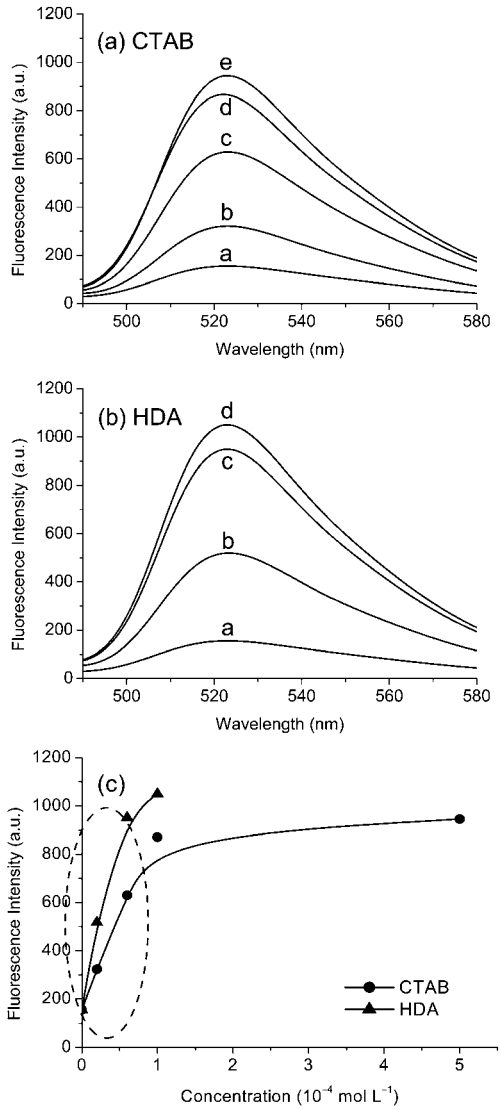

Fig. 9 Fluorescence spectra of calcein released from the CB[7]-threaded, 1,4-butanediamine-modified MCM-41 systems in aqueous solutions in the presence of competitors at equilibrium: (a) CTAB/10^{-4} mol L^{-1}; a) 0.0; b) 0.2; c) 0.6; d) 1.0; e) 1.0; (b) 1,6-hexanediamine (HDA)/10^{-4} mol L^{-1}; a) 0.0; b) 0.2; c) 0.6; d) 1.0; (c) emission intensity of calcein as a function of competitor concentration.

solutions even at pH 6.5, some dissociation would take place, leading to sustained calcein release albeit probably slow. This could be prevented by adding some CB[7] to the buffer solutions. The controlled releases for the buffer solutions with and without CB[7] are compared here at pH 6.5 before triggered release (Fig. S3†). The emission intensity of calcein grew slightly with time in the absence of CB[7], instead of remaining unchanged. In the presence of CB[7] (at the concentration of 1×10^{-9} mol L^{-1}), the leakage was inhibited, which can be regarded as the reverse process of the controlled release by competitive binding. It is obvious that the buffer solution containing a small amount of CB[7] could effectively block the nanopores and resulted in no leakage before triggered release. Taking into account the time-scale of the controlled release here, no significant influence occurred without addition of CB[7]. The addition of CB[7] would improve the nanovalve effect in the case of sustained release over a long period.

By combination of the two stimuli under various conditions (pH, competitors, and concentrations), the release rates and amounts of entrapped molecules through the nanovalve operation could be varied on demand to meet different requirements (rapid and sustained releases). It is possible that targeted release of drug molecules entrapped in the MCM-41 supports through the CB[7]-based nanovalves can be realized for some tissues and organs in basic environments or in the presence of biologically relevant cationic species under physiological conditions.

Conclusions

In summary, the controlled release of the supramolecular nanovalves of CB[7]-threaded, 1,4-butanediamine-modified MCM-41 supports driven by dual stimuli was investigated in detail. The encirclement of CB[7] onto the protonated 1,4-butanediamine stalks anchored on the MCM-41 surfaces led to the tight closing of nanopores. The closed pores could be opened by deprotonation and competitive binding in aqueous solutions, so that the entrapped calcein molecules were released from the pore voids into bulk solution. The closing and opening of the supramolecular nanovalves were easily observed from the changes in fluorescence intensity of calcein and in color of suspended solutions. The increase of pH led to the deprotonation of the initially protonated 1,4-butanediamine units and the dissociation of the supramolecular complexes, and the amount of released calcein increased with increasing pH. The competitors CTAB and 1,6-hexanediamine could activate the nanovalves through the shift of the supramolecular complex equilibrium. The increases in binding affinity and concentration of the competitors gave rise to an increase in release rate and efficiency. In addition, the dimension of the movable elements and their binding affinity to the anchored stalks had an influence on nanovalve leakage and release efficiency. The controlled release of the supramolecular nanovalves driven by deprotonation and competitive binding under various conditions could be finely tuned on demand and will have many potential applications in different fields, such as nanocarriers, molecular machines, and fluorescence sensors.

Acknowledgements

This work was supported by the National Natural Science Foundation of China (No. 20873062) and the program for New Century Excellent Talents in University (NCET-07-0412).

References

1 W. J. Rieter, K. M. Pott, K. M. L. Taylor and W. Lin, *J. Am. Chem. Soc.*, 2008, **130**, 11584–11585.
2 Y.-Z. You, K. K. Kalebaila, S. L. Brock and D. Oupicky, *Chem. Mater.*, 2008, **20**, 3354–3359.
3 S. C. Lee, C. Kim, I. C. Kwon, H. Chung and S. Y. Jeong, *J. Controlled Release*, 2003, **89**, 437–446.
4 R. B. Greenwald, K. Yang, H. Zhao, C. D. Conover, S. Lee and D. Filpula, *Bioconjugate Chem.*, 2003, **14**, 395–403.
5 C.-Y. Hong, X. Li and C.-Y. Pan, *J. Mater. Chem.*, 2009, **19**, 5155–5160.
6 C. Liu, J. Guo, W. Yang, J. Hu, C. Wang and S. Fu, *J. Mater. Chem.*, 2009, **19**, 4764–4770.

7 A. V. Ambade, E. N. Savariar and S. Thayumanavan, *Mol. Pharmaceutics*, 2005, **2**, 264–272.
8 J.-H. Yang, Y.-S. Han, M. Park, T. Park, S.-J. Hwang and J.-H. Choy, *Chem. Mater.*, 2007, **19**, 2679–2685.
9 C.-Y. Lai, B. G. Trewyn, D. M. Jeftinija, K. Jeftinija, S. Xu, S. Jeftinija and V. S.-Y. Lin, *J. Am. Chem. Soc.*, 2003, **125**, 4451–4459.
10 B. G. Trewyn, C. M. Whitman and V. S.-Y. Lin, *Nano Lett.*, 2004, **4**, 2139–2143.
11 F. Balas, M. Manzano, P. Horcajada and M. Vallet-Regi, *J. Am. Chem. Soc.*, 2006, **128**, 8116–8117.
12 E. Aznar, M. D. Macros, R. Martinez-Manez, F. Sancenon, J. Soto, P. Amoros and C. Guillem, *J. Am. Chem. Soc.*, 2009, **131**, 6833–6843.
13 P. Yang, Z. Quan, L. Lu, S. Huang and J. Lin, *Biomaterials*, 2008, **29**, 692–702.
14 Y. Liu, W. Zhang and T. Pinnavaia, *Angew. Chem., Int. Ed.*, 2001, **40**, 1255–1258.
15 Y. Han, D. Li, L. Zhao and F. Xiao, *Angew. Chem., Int. Ed.*, 2003, **42**, 3633–3637.
16 C. Barbe, J. Bartlett, L. Kong, K. Finnie, H. Q. Lin, M. Larkin, S. Calleja, A. Bush and G. Calleja, *Adv. Mater.*, 2004, **16**, 1959–1966.
17 E. J. Kwon and T. G. Lee, *Appl. Surf. Sci.*, 2008, **254**, 4732–4737.
18 F. Hoffmann, M. Corenlius, J. Morell and M. Froba, *Angew. Chem., Int. Ed.*, 2006, **45**, 3216–3251.
19 S. Huh, J. W. Wiench, J. C. Yoo, M. Pruski and V. S.-Y. Lin, *Chem. Mater.*, 2003, **15**, 4247–4256.
20 B. G. Trewyn, I. I. Slowing, S. Giri, H. Chen and V. S.-Y. Lin, *Acc. Chem. Res.*, 2007, **40**, 846–853.
21 R. Casasus, E. Aznar, M. D. Marcos, R. Martinez-Manez, F. Sancenon, J. Soto and P. Amoros, *Angew. Chem., Int. Ed.*, 2006, **45**, 6661–6664.
22 Y. Zhao, B. G. Trewyn, I. I. Slowing and V. S.-Y. Lin, *J. Am. Chem. Soc.*, 2009, **131**, 8398–8400.
23 N. K. Mal, M. Fujiwara and Y. Tanaka, *Nature*, 2003, **421**, 350–353.
24 N. K. Mal, M. Fujiwara, Y. Tanaka, T. Taguchi and M. Matsukata, *Chem. Mater.*, 2003, **15**, 3385–3394.
25 S. Angelos, E. Choi, F. Vogtle, L. De Cola and J. I. Zink, *J. Phys. Chem. C*, 2007, **111**, 6589–6592.
26 E. Aznar, R. Casasus, B. Garcia-Acosta, M. D. Marcos, R. Martinez-Manez, F. Sancenon, J. Soto and P. Amoros, *Adv. Mater.*, 2007, **19**, 2228–2231.
27 R. Casasus, E. Climent, M. D. Marcos, R. Martinez-Manez, F. Sancenon, J. Soto, P. Amoros, J. Cano and E. Ruiz, *J. Am. Chem. Soc.*, 2008, **130**, 1903–1917.
28 T. D. Nguyen, Y. Liu, S. Saha, K. C.-F. Leung, J. F. Stoddart and J. I. Zink, *J. Am. Chem. Soc.*, 2007, **129**, 626–634.
29 C. Park, K. Oh, S. C. Lee and C. Kim, *Angew. Chem., Int. Ed.*, 2007, **46**, 1455–1457.
30 S. Giri, B. G. Trewyn, M. P. Stellmaker and V. S.-Y. Lin, *Angew. Chem., Int. Ed.*, 2005, **44**, 5038–5044.
31 F. Torney, B. G. Trewyn, V. S.-Y. Lin and K. Wang, *Nat. Nanotechnol.*, 2007, **2**, 295–300.
32 K. C.-F. Leung, T. D. Nguyen, J. F. Stoddart and J. I. Zink, *Chem. Mater.*, 2006, **18**, 5919–5628.
33 T. D. Nguyen, K. C.-F. Leung, M. Liong, C. D. Pentecost, J. F. Stoddart and J. I. Zink, *Org. Lett.*, 2006, **8**, 3363–3366.
34 K. Patel, S. Angelos, W. R. Dichtel, A. Coskun, Y.-W. Yang, J. I. Zink and J. F. Stoddart, *J. Am. Chem. Soc.*, 2008, **130**, 2382–2383.
35 R. Hernandez, H.-R. Tseng, J. W. Wong, J. F. Stoddart and J. I. Zink, *J. Am. Chem. Soc.*, 2004, **126**, 3370–3371.
36 S. Angelos, Y. Yang, K. Patel, J. F. Stoddart and J. I. Zink, *Angew. Chem., Int. Ed.*, 2008, **47**, 2222–2226.
37 S. Angelos, M. Liong, E. Choi and J. I. Zink, *Chem. Eng. J.*, 2008, **137**, 4–13.
38 H. Lin, G. Zhu, J. Xing, B. Gao and S. Qiu, *Langmuir*, 2009, **25**, 10159–10164.
39 J. Lagona, P. Mukhopadhyay, S. Chakrabarti and L. Isaacs, *Angew. Chem., Int. Ed.*, 2005, **44**, 4844–4870.
40 K. Kim, N. Selvapalam, Y. H. Ko, K. M. Park, D. Kim and J. Kim, *Chem. Soc. Rev.*, 2007, **36**, 267–279.
41 J. W. Lee, S. Samal, N. Selvapalam, H.-J. Kim and K. Kim, *Acc. Chem. Res.*, 2003, **36**, 621–630.
42 J. Mohanty and W. M. Nau, *Angew. Chem., Int. Ed.*, 2005, **44**, 3750–3754.
43 Y. Ling, W. Wang and A. E. Kaifer, *Chem. Commun.*, 2007, 610–612.
44 R. Wang, L. Yuan and D. H. Macartney, *Chem. Commun.*, 2005, 5867–5869.
45 T. A. Martyn, J. L. Moore, R. L. Halterman and W. T. Yip, *J. Am. Chem. Soc.*, 2007, **129**, 10338–10339.
46 A. Henning, H. Bakirci and W. M. Nau, *Nat. Methods*, 2007, **4**, 629–632.
47 C. Marquez, F. Huang and W. M. Nau, *IEEE Trans. NanoBiosci.*, 2004, **3**, 39–45.
48 C. T. Kresge, M. E. Leonowicz, W. J. Roth, J. C. Vartuli and J. S. Beck, *Nature*, 1992, **359**, 710–712.
49 J. Kim, I.-S. Jung, S.-Y. Kim, E. Lee, J.-K. Kang, S. Sakamoto, K. Yamaguchi and K. Kim, *J. Am. Chem. Soc.*, 2000, **122**, 540–541.
50 W. L. Mock and N. Y. Shih, *J. Org. Chem.*, 1986, **51**, 4440–4446.
51 Y. H. Ko, H. Kim, Y. Kim and K. Kim, *Angew. Chem., Int. Ed.*, 2008, **47**, 4106–4109.
52 S. Liu, C. Ruspic, P. Mukhopadhyay, S. Chakrabarti, P. Y. Zavalij and L. Isaacs, *J. Am. Chem. Soc.*, 2005, **127**, 15959–15967.